

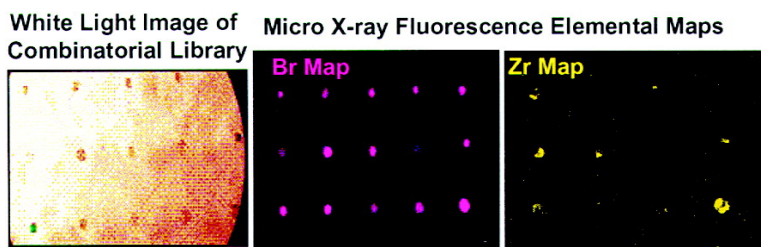
Article

## Micro-X-ray Fluorescence as a General High-Throughput Screening Method for Catalyst Discovery and Small Molecule Recognition

Thomasin C. Miller, Grace Mann, George J. Havrilla, Cyndi A. Wells, Benjamin P. Warner, and R. Tom Baker

*J. Comb. Chem.*, **2003**, 5 (3), 245-252 • DOI: 10.1021/cc020102g • Publication Date (Web): 28 February 2003

Downloaded from <http://pubs.acs.org> on March 20, 2009



### More About This Article

Additional resources and features associated with this article are available within the HTML version:

- Supporting Information
- Links to the 2 articles that cite this article, as of the time of this article download
- Access to high resolution figures
- Links to articles and content related to this article
- Copyright permission to reproduce figures and/or text from this article

[View the Full Text HTML](#)

# Micro-X-ray Fluorescence as a General High-Throughput Screening Method for Catalyst Discovery and Small Molecule Recognition

Thomasin C. Miller, Grace Mann, George J. Havrilla,\* Cyndi A. Wells,  
Benjamin P. Warner, and R. Tom Baker

*Los Alamos National Laboratory, Chemistry Division, Mail Stop K484, Los Alamos, New Mexico 87545*

*Received November 20, 2002*

A powerful high-throughput screening technique is described for the rapid screening of bead-based libraries for catalyst discovery and molecular recognition. Micro-X-ray fluorescence (MXRF) screens materials for elemental composition with mesoscale analysis. This method is nondestructive and requires minimal sample preparation and no special tags for analysis, and the screening time is dependent on the desired sensitivity. The speed, sensitivity, and simplicity of MXRF as a high-throughput screening technique were applied to screen bead-based libraries of oligopeptides for phosphate hydrolysis catalysts and molecular recognition of selective receptors for the degradation products and analogues of chemical warfare agents. This paper demonstrates the analytical or HTS capability of MXRF for combinatorial screening. It is meant only to show the capabilities of MXRF and is not meant as an exhaustive study of the catalyst and molecular recognition systems presented.

## Introduction

Combinatorial chemistry has revolutionized the synthesis of compounds on solid supports, but the major bottleneck of this process is the reliable and rapid screening of desired properties of resin-bound components.<sup>1</sup> Whether it is for the combinatorial development of new drugs, catalysts, or molecular receptors, the activity and selectivity of library components have to be determined quickly and reliably. The ideal method for screening would be on-bead reaction monitoring. Active research in this area has led to recent discoveries in high-throughput screening (HTS) methods based on mass spectrometry,<sup>2–4</sup> infrared thermography,<sup>5</sup> Fourier transform infrared spectroscopy,<sup>6–10</sup> near-infrared spectroscopy,<sup>11,12</sup> laser-induced resonance-enhanced multiphoton excitation,<sup>13</sup> and laser-induced fluorescence imaging.<sup>14</sup> Building on these successes, a novel means of molecular recognition using a solid-supported combinatorial technique and elemental screening method is described in this study.

X-ray detection techniques have previously been applied in combinatorial analyses. For example, synchrotron microbeam-XRF was applied to characterize the composition of a library of rare earth activated Gd (La, Sr) AlO<sub>3</sub> phosphor thin films.<sup>15</sup> Energy-dispersive X-ray spectroscopy on a scanning electron microscope has been used to analyze organic compounds on single library beads (typically 50 μm in diameter).<sup>16,17</sup> Additionally, X-ray photoelectron spectroscopy has been used to analyze bead-supported reactions.<sup>18,19</sup> Even though X-ray fluorescence (XRF) and similar techniques have been routine means of elemental analysis for the last 25 years, the primary advantage of micro-X-ray

fluorescence (MXRF) is the ability to fill the gap between bulk elemental analysis (tens of square millimeters) by XRF and high-resolution elemental determinations (<10 μm<sup>2</sup>) by scanning electron microscopy, secondary ion mass spectrometry, and synchrotron-based technologies. Mesoscale (>10 μm<sup>2</sup>) analysis is achieved through the use of a polycapillary focusing optic in conjunction with a Rh X-ray tube source, which focuses the source X-rays into a nominal spot size of 30–50 μm in diameter. MXRF has been used for high-throughput experimentation<sup>20</sup> as well as for combinatorial library development.<sup>21</sup> Like conventional XRF, MXRF can detect elemental composition for a given sample by measuring its characteristic X-ray emission wavelengths or energies. A schematic representation of the MXRF instrument is shown in Figure 1. MXRF allows for simultaneous elemental analysis with both quantitative and qualitative analysis of elements Z ≥ 11. It is a nondestructive technique that identifies and quantifies elements on solid supports with minimal sample preparation. Three types of analyses can be performed with MXRF to provide unique elemental information about a given sample: single point analyses, linescans, and elemental imaging. Spatially resolved qualitative and quantitative information can be gained through spectra acquired by single-point analysis between different samples and varying locations on the same sample. Linescans give qualitative information, such as elemental concentration gradients across a sample surface. Elemental imaging allows for qualitative and quantitative information about sample heterogeneity or for the direct comparison of elemental intensities either within a sample or between different samples in a single experiment.

MXRF is also unique, as compared with detection techniques, such as fluorescence, UV, and other techniques often used in molecular recognition, in that it detects the

\* Corresponding author. Tel: 1-505-667-9627. Fax: 1-505-665-5982.  
E-mail: havrilla@lanl.gov.

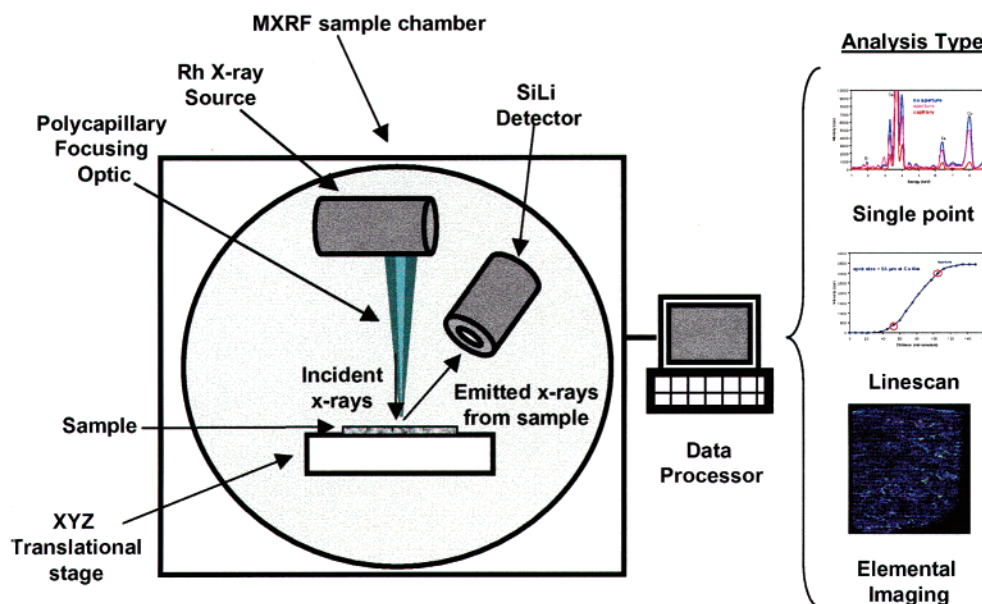


**Figure 1.** Schematic representation of MXRF instrumentation.

native elemental fluorescence signature of the combinatorial reaction species. Techniques such as molecular fluorescence require that the molecules of interest be naturally fluorescent, limiting the range of reactants, or that the molecules contain a fluorescent tag. Added tags are often bulky and can adversely interfere, both sterically and chemically, with the specific molecular recognition chemistry. Furthermore, fluorescent tags undergo rapid photobleaching when measurements are performed with high spatial resolution similar to MXRF. MXRF avoids this problem, since the method does not require added tags. However, MXRF does require that a detectable heteroatom,  $Z \geq 11$ , be present for analysis.

This paper investigates the use of MXRF as a high-throughput screening method for analyzing a combinatorial library of standard polystyrene resin beads of oligopeptides for catalytic activity as well as molecular recognition of small molecules. Specifically, the first study involved screening a library for potential catalysts consisting of peptide sequences that have the ability to catalyze phosphate hydrolysis in the presence of a Lewis acid. Second, MXRF was used to screen a peptide library of potential molecular receptors for the degradation products and analogues of the chemical warfare organophosphate nerve agent VX.

### Experimental Section

**Materials.** All reagents were commercially available and used without further purification. Solid-supported oligopeptides and libraries of oligopeptides were used with protecting groups removed and were acquired from Biopeptide Inc. LLC (San Diego, CA). 5-Bromo-4-chloroindolyl phosphate (BCP) **1** and 4-(2-hydroxyethyl)-1-piperazinepropanesulfonic acid (EPPS) **2** were purchased from Acros Organics (Belgium). Zirconium(IV) chloride **3** and methylphosphonic acid **4** were obtained from Aldrich Chemical Corporation (St. Louis, MO). 2-Diethylaminoethanethiol hydrochloride **5** was obtained from Fluka Chemical (Switzerland). Tacky Dot array slides were purchased from SPI Supplies (Westchester, PA).

**Instrumentation.** X-ray excitation and detection were performed using an EDAX Eagle II micro-X-ray fluorescence

**Table 1.** Element Emission Lines and Energies Monitored in This Study.

element	emission line	emission line energy (keV)
Br	K-L <sub>2,3</sub> (K $\alpha$ )	11.91
Ca	K-L <sub>2,3</sub> (K $\alpha$ )	3.69
Cl	K-L <sub>2,3</sub> (K $\alpha$ )	2.62
P	K-L <sub>2,3</sub> (K $\alpha$ )	2.01
S	K-L <sub>2,3</sub> (K $\alpha$ )	2.31
Zr	K-L <sub>2,3</sub> (K $\alpha$ )	15.74
Zr	L-M <sub>4,5</sub> (L $\alpha$ )	2.04

system equipped with a Rh target excitation source and a SiLi detector (EDAX, Mahwah, NJ). The X-ray source was equipped with a polycapillary focusing optic having a 50- $\mu\text{m}$  nominal X-ray spot size (X-ray Optical Systems, Albany, NY). X-ray tube operating conditions were maintained at 35 kV and 400  $\mu\text{A}$  during all analyses. The matrix chosen for each image was 128  $\times$  100 pixels with a 200-ms dwell time per pixel. A typical imaging time for a Tacky Dot array of beads was 1 h. Individual beads were mapped in 15 min. The integration time of individual spectra was 100 live detector seconds. A schematic representation of the instrument is shown in Figure 1. Table 1 lists the element emission lines and their energies that were monitored in the experiments outlined in this study. Microscope observation was performed on a Leica Micro Star IV stereomicroscope (Leica Microsystems, Bannockburn, IL).

Edman degradation experiments were determined by the Molecular Biology Core Facility at Dartmouth University on a PE/ABI model 476A protein sequencer (Applied Biosystems, Foster City, CA). MALDI analysis was performed on a Voyager System 4147 (Applied Biosystems.)

**Procedures.** *Screening of Oligopeptide Library for Phosphate Hydrolysis Catalysts.* Approximately 20 mg ( $\sim$ 12 500 beads) of a Wang resin-bound 11-mer oligopeptide combinatorial library was immersed in an aqueous solution of **3** (0.3 mL, 69 mM, pH 2.0) for 48 h with frequent mixing. After exposure, the beads were isolated from the reaction solution by gravity filtration, rinsed three times with 5 mL of deionized water, and air-dried for 12 h on filter paper.

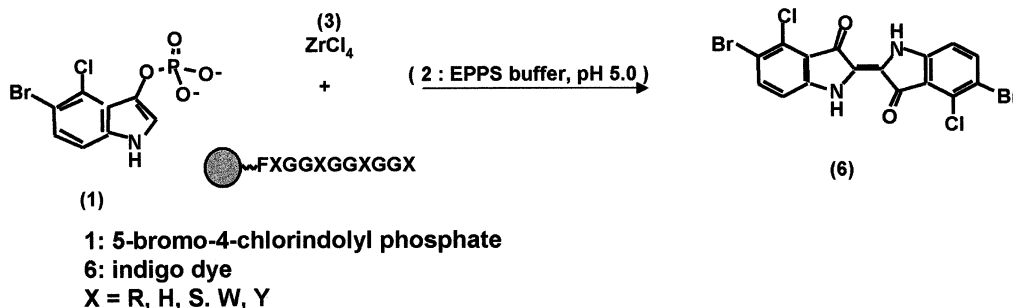


**Figure 2.** Hydrolysis and oxidation of **1** with potential oligopeptide combinatorial library catalysts in the presence of buffered  $Zr^{4+}$  acting as a Lewis acid to form **6**.

The beads were then exposed to an aqueous solution (pH 5.0) of **3** (0.3 mL, 8.6 mM), **1** (0.3 mL, 5.4 mM), and **2** (0.4 mL, 320 mM). The beads were allowed to react in this solution for 24 h with frequent mixing. The beads were then isolated by gravity filtration, rinsed three times with 5 mL of deionized water, and air-dried for 12 h on filter paper. Another 20-mg sample of library beads was exposed to deionized water (0.8 mL) for both reaction cycles as a control.

The dried beads were then immobilized onto and spatially separated from one another on a Tacky Dot array plate, then imaged with MXRF. Screening time was 1 h per Tacky Dot plate (~3200 immobilized beads). Specifically, the Br K- $L_{2-3}$  ( $K\alpha$ ), Ca K- $L_{2-3}$  ( $K\alpha$ ), Cl K- $L_{2-3}$  ( $K\alpha$ ), P K- $L_{2-3}$  ( $K\alpha$ ), Zr K- $L_{2-3}$  ( $K\alpha$ ), and Zr L- $M_{2-3}$  ( $L\alpha$ ) X-ray emission lines were monitored to detect beads that hydrolyzed product. Two beads were isolated, and their amino acid sequences were determined by Edman degradation. Resin-bound oligopeptides of these sequences were purchased, and the beads were subjected to reaction conditions, similar to those described for the library of beads, and imaged with MXRF to verify their catalytic activity.

*Screening of Oligopeptide Library for Molecular Receptors.* Approximately 20 mg of the Wang resin-bound 11-mer oligopeptide combinatorial library was exposed to an aqueous solution of **4** (0.2 mL, 180 mM), **5** (0.2 mL, 180 mM), and deionized water (0.4 mL) for 48 h with frequent mixing to effect library/target binding. Another 20-mg sample of library beads was exposed to deionized water (0.8 mL) for 48 h as a control. After exposure, the beads were isolated from the reaction solution by gravity filtration, rinsed three times with deionized water (5 mL), and air-dried for 12 h on filter paper.

The library of beads were then immobilized onto a Tacky Dot array plate and imaged by MXRF. The PK $\alpha$  and SK $\alpha$  X-ray emission lines were monitored to detect the P from **4** and the S from **5** for small molecule recognition. Two beads were isolated, and their amino acid sequence was determined by Edman degradation. Resin-bound oligopeptides of these sequences were purchased and the beads were subjected to reaction conditions similar to those described for the library of beads and imaged with MXRF to verify their molecular recognition abilities. The beads from the control sample showed no significant P or S signal, indicating the deionized water did not contain any experimental interfering agents.

## Results and Discussion

**Screening of Oligopeptide Library for Phosphate Hydrolysis Catalysts.** The bead-based library chosen by Berkessel and Herauld for the discovery of phosphate hydrolysis catalysts<sup>22</sup> was used in this study to demonstrate the feasibility of MXRF as a combinatorial library-screening technique. A library of 625 solid-supported oligopeptides whose sequence is resin-FXGGXGGXGGX, where X is arginine (R), histidine (H), serine (S), tryptophan (W), or tyrosine (Y), G is glycine, and F is phenylalanine, was purchased. Each bead in the library is ~100  $\mu$ m in diameter and contains only one type of sequence attached to it. Prior to performing the phosphate hydrolysis reaction, the library beads were initially pretreated with  $ZrCl_{4(aq)}$ , which was found experimentally to ensure the absorption of Zr to the catalytically active sequences. Figure 2 shows the phosphate hydrolysis reaction of **1** with the oligopeptide library in the presence of Lewis acid **3** and buffer **2**. Catalytic sequences will facilitate the hydrolysis of the O–P bond in the presence of  $Zr^{4+}$ , forming an enol that undergoes air oxidation to form an insoluble indigo dye **6**, which precipitates on the bead and can be visibly detected.

After exposure to a buffered solution of  $Zr^{4+}$  and **1**, the library arrays were screened by MXRF for the presence of Br, P, and Zr to determine which beads, that is, peptide sequences, were good phosphate hydrolysis catalysts. Figure 3 displays the hydrolysis MXRF maps of Br, Ca, Cl, P, and Zr as well as the white light image from the microscope of a small number of reacted beads on the Tacky Dot array. For each elemental map, colored “hot spots” represent the presence of that element on the bead, and the intensity of the colors roughly corresponds to the abundance of that element. The Ca map is the elemental distribution of Ca in the glass slide. Calcium is not present in the library beads; therefore, the Ca map shows the beads on the glass slide giving dark areas in the Ca elemental map. The uniform distribution shown on the Cl map is indicative of  $Cl^-$  from the  $ZrCl_4$  solution, which appears to be associated with all of the peptides. A control experiment was run to verify that the Cl bound to the beads was only from the  $ZrCl_4$  and not from any other reactants or products of the phosphate hydrolysis reaction. In contrast, the Br, P, and Zr maps show dramatic differences in intensity and, thus, abundance of each element on each bead. Beads 1, 2, 6, 8, 9, 10, 11, and 13 show hot spots for Br. In comparison with the P map, beads

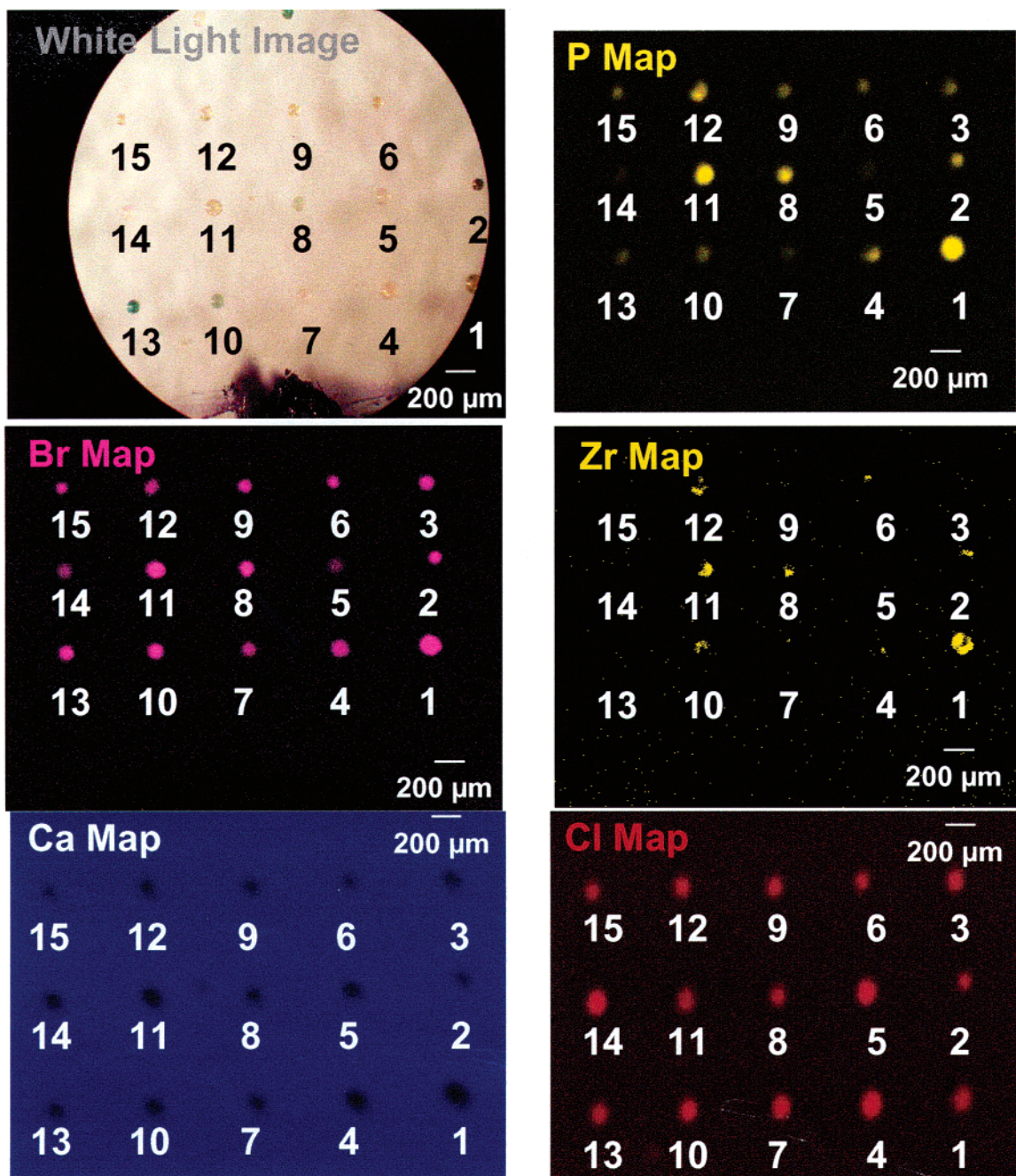


**Figure 3.** Microscope white light image with the MXRF elemental maps of Br, Ca, Cl, P, and Zr of oligopeptide library beads previously exposed to phosphate hydrolysis reaction conditions. For each elemental map, colored “hot spots” represent the presence of that element on the bead, and the intensity of the colors roughly corresponds to the abundance of that element. Bead 13 is dark blue in color with a high Br intensity and low P and Zr intensities, indicating that it is a good phosphate hydrolysis catalyst. Bead 10, a moderate catalyst, is a light blue bead with significant Br and Zr intensities. Beads 1, 8, 11, and 12 have significant Br and P intensities, indicating that these beads have bound **1**.

1, 8, 11, and 12 show high intensity for P, indicating the presence of the starting material, since **1** contains P and Br on the same molecule. Additionally, the beads high in P could have also bound the phosphoric acid byproduct of the hydrolysis reaction. In contrast, beads 10 and 13 are light blue and dark blue, respectively, indicating the hydrolysis reaction was catalyzed by these beads. The MXRF images show that the dark blue bead has a strong Br intensity with minimal Zr and P, indicating the loss of phosphate from the starting material **1** to form **6**, and thus, it is a good catalyst. The light blue bead has a strong Br intensity as well as a

moderate Zr signal, indicating it is only a moderate catalyst for the hydrolysis reaction.

This study demonstrates that MXRF can be used to distinguish between beads that bind the indolyl phosphate starting material, Zr Lewis acid, phosphoric acid byproduct, or some combination thereof, as well as discern which library beads are active for phosphate hydrolysis. MXRF can also be used to determine how a particular analyte is interacting with a particular library bead. For example, Figure 4 shows high-resolution MXRF maps of  $Zr^{4+}$  bound to beads 1, 4, 7, 10, and 13, which indicates specific coordination of  $Zr^{4+}$  to

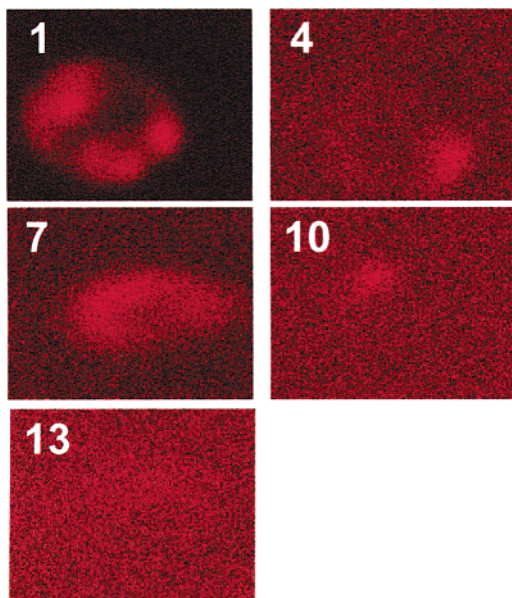


**Figure 4.** High-resolution MXRF elemental Zr maps of library beads 1, 4, 7, 10, and 13.

the peptides on the beads. It is clear that the Zr is not uniformly distributed over the bead and is associated with the peptide bound to the surface. Preliminary studies of Zr uptake onto the beads suggest that low nanogram quantities of material are present on the beads and can easily be detected by MXRF.

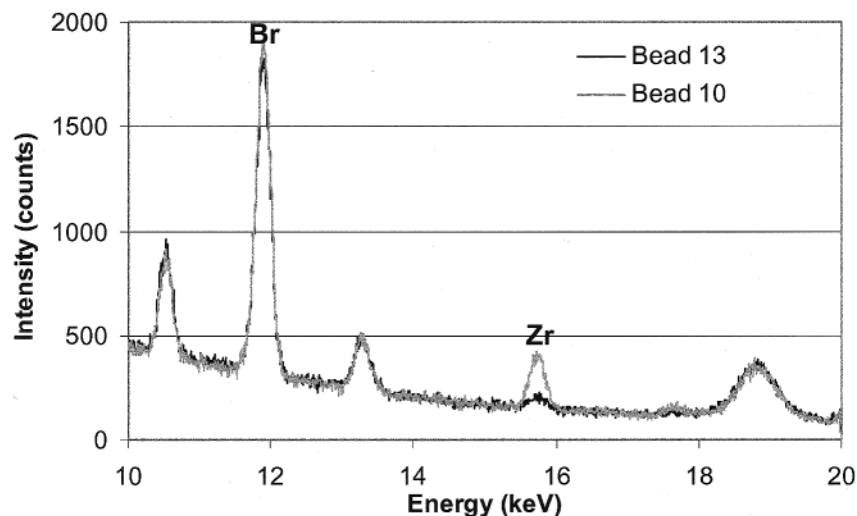
The catalyst efficiency for a particular bead sequence can also be determined from the X-ray fluorescence spectra obtained by MXRF. The X-ray fluorescence spectra of beads 10 and 13 are shown in Figure 5. From the spectra, the Br/Zr intensity ratio can be obtained for each bead. The Br and Zr intensities are listed in Table 2. Bead 13, which is the dark blue bead, shows the largest Br/Zr ratio and, thus, is a very efficient catalyst, because a large amount of **6** is present on the bead. Bead 10, which is a lighter blue, has a smaller Br/Zr ratio than bead 13 and is a less efficient catalyst. Beads 10 and 13 were then removed, and their sequences were determined by Edman degradation and listed in Table 2. These specific immobilized oligopeptides were then independently subjected to phosphate hydrolysis conditions, and

their catalytic ability in the presence of  $Zr^{4+}$  was verified. The overall Br and Zr intensities for 10 different beads of sequences 10 and 13 are shown in Table 2. MXRF verified that beads containing catalyst sequence 13 act as good catalysts with a high Br/Zr ratio, but the beads containing sequence 10 act as a moderate catalyst with a lower Br/Zr ratio. Therefore, MXRF can be used both for the initial library screen and subsequent verification of potential catalysts.

Like the optical analysis performed by Berkessel and Herault,<sup>22</sup> MXRF was used to find combinatorial library beads that acted as catalysts for phosphate hydrolysis. In his study, Berkessel found three catalytically active oligopeptide sequences. These sequences only contained G, H, R, and S amino acid residues. For the two bead sequences determined by MXRF, the sequence for bead 10 SGGHGGRGGHF (the moderate catalyst) matched directly with an active sequence found by Berkessel. The sequence found for bead 13 was different from the three sequences found by Berkessel. However, like those found by Berkessel, the sequence contained only G, H, R, and S amino acid residues. These results uphold Berkessel's assumption that combinations of H and S may be the common feature of active sequences. However, it should be understood that this study is not meant to be an exhaustive comparison with Berkessel, but is a demonstration of MXRF as a HTS application to a catalytic system. This paper demonstrates the analytical or HTS capability of MXRF for combinatorial screening.

Unlike the optical technique presented by Berkessel, MXRF has the capability to study other chemistries that may be taking place on library beads that cannot be detected optically. For example, MXRF has the capability to detect sequences that bind only Zr and do not participate in the phosphate hydrolysis reaction. Such sequences could, for example, be used as Zr sequestration agents from water waste streams.

**Screening of Oligopeptide Library for Small Molecule Molecular Recognition.** As part of the ongoing research into small molecule recognition, the degradation products of the organophosphate chemical nerve agent VX were chosen as the targets of interest for receptor discovery. Both the

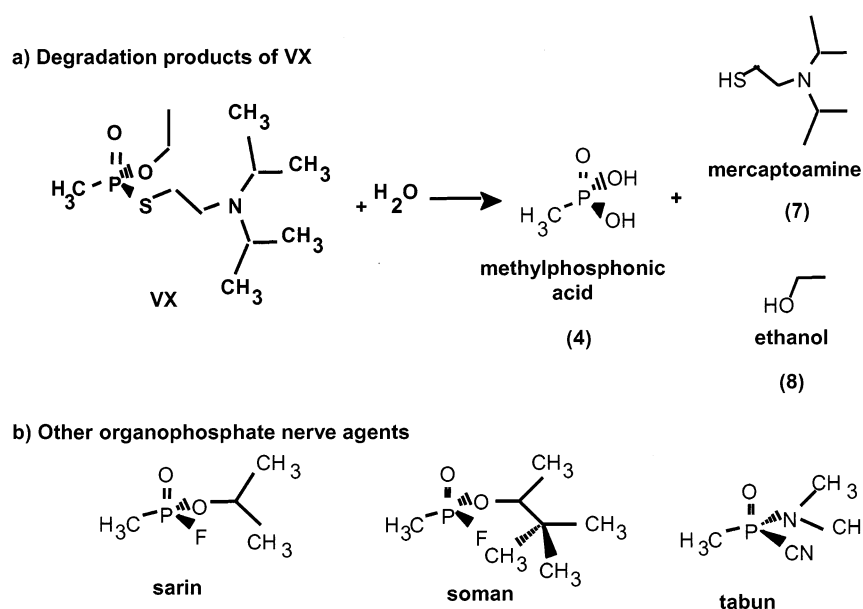


**Figure 5.** MXRF spectra of catalyst beads 10 and 13. Spectral live time = 100 s.

**Table 2.** MXRF P, Br, and Zr Intensities of Catalyst Beads 1–15 from the Original Screen and Intensities and Peptide Sequences as Determined from the Verification Experiments.

bead <sup>a</sup>	original screen: intensity (counts), (n = 1)			sequence	verification: intensity (counts), (n = 10)		
	P	Br	Zr		P	Br	Zr
1	4090	1619	873	N/A	N/A	N/A	N/A
2	2012	1900	193	N/A	N/A	N/A	N/A
3	401	937	30	N/A	N/A	N/A	N/A
4	620	889	33	N/A	N/A	N/A	N/A
5	231	513	46	N/A	N/A	N/A	N/A
6	975	1477	73	N/A	N/A	N/A	N/A
7	707	981	30	N/A	N/A	N/A	N/A
8	4397	1917	236	N/A	N/A	N/A	N/A
9	962	1669	47	N/A	N/A	N/A	N/A
10	715	1611	239	SGGHGGRGGHF	1362 ± 712	624 ± 177	141 ± 45
11	6293	1622	808	N/A	N/A	N/A	N/A
12	3496	1260	410	N/A	N/A	N/A	N/A
13	736	1485	28	SGGHGGRGGRF	865 ± 264	784 ± 267	66 ± 19
14	612	585	27	N/A	N/A	N/A	N/A
15	998	698	49	N/A	N/A	N/A	N/A

<sup>a</sup> Bead numbers are equivalent to those shown and labeled in Figure 3.

**Figure 6.** Structures of (a) VX and hydrolysis degradation products and (b) other organophosphate nerve agents.

structure of VX and the structures of other similar agents are shown in Figure 6. This class of nerve agents acts to inhibit acetylcholinesterase, an enzyme used in the degradation pathway of the neurotransmitter, acetylcholine, in biological systems. These agents irreversibly bind to the acetylcholinesterase, resulting in perpetual nerve cell stimulation leading to severe incapacitation or even death to the exposed organism.<sup>23</sup> The degradation scheme of VX is illustrated in Figure 6a. VX rapidly hydrolyses in the presence of water to **4**, diisopropylaminoethyl mercaptan **7**, and ethanol **8**. Methylphosphonic acid is a product common to most organophosphate nerve agents, whereas **7** is unique to VX. Figure 7 shows the reaction scheme of the peptide library with the VX degradation product targets. Upon exposure to the degradation products, four distinct types of interaction are possible. A library sequence can bind individually to **4** or **7**. Both targets could bind to a particular sequence, or no interaction could take place at all. An analogue of the actual mercaptoamine degradation product,

**5**, was chosen for this study because of its commercial availability.

After exposure to the VX degradation product targets, the library of oligopeptides was screened by MXRF for the presence of phosphorus or sulfur, which would indicate the presence of bound VX degradation products **4** and **5** to library beads. Figure 8 displays the P, S, Cl, and P/S overlay MXRF maps of the exposed array of library beads. The P map shows the beads in the array that bound **4**, while the S map shows the beads that bound **5**. The initial goal of this screen was to determine oligopeptides that showed both strong affinity for both degradation products and, thus, would be good candidates for receptors for CW agents. Two beads that fit these characteristics were selected from the library. The bead labeled “1” gave the most significant counts in the P map as well as minimal counts for S. Similarly, bead “2” strongly bound S with minimal P. Bead “3” bound neither P nor S and displayed no significant Cl intensity. The overall Cl, P, and S counts for each of these beads are listed in Table 3,

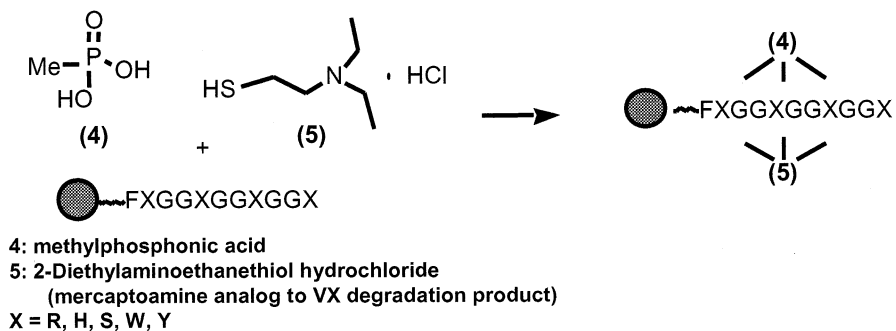


Figure 7. Reaction scheme of VX degradation products with the oligopeptide combinatorial library.

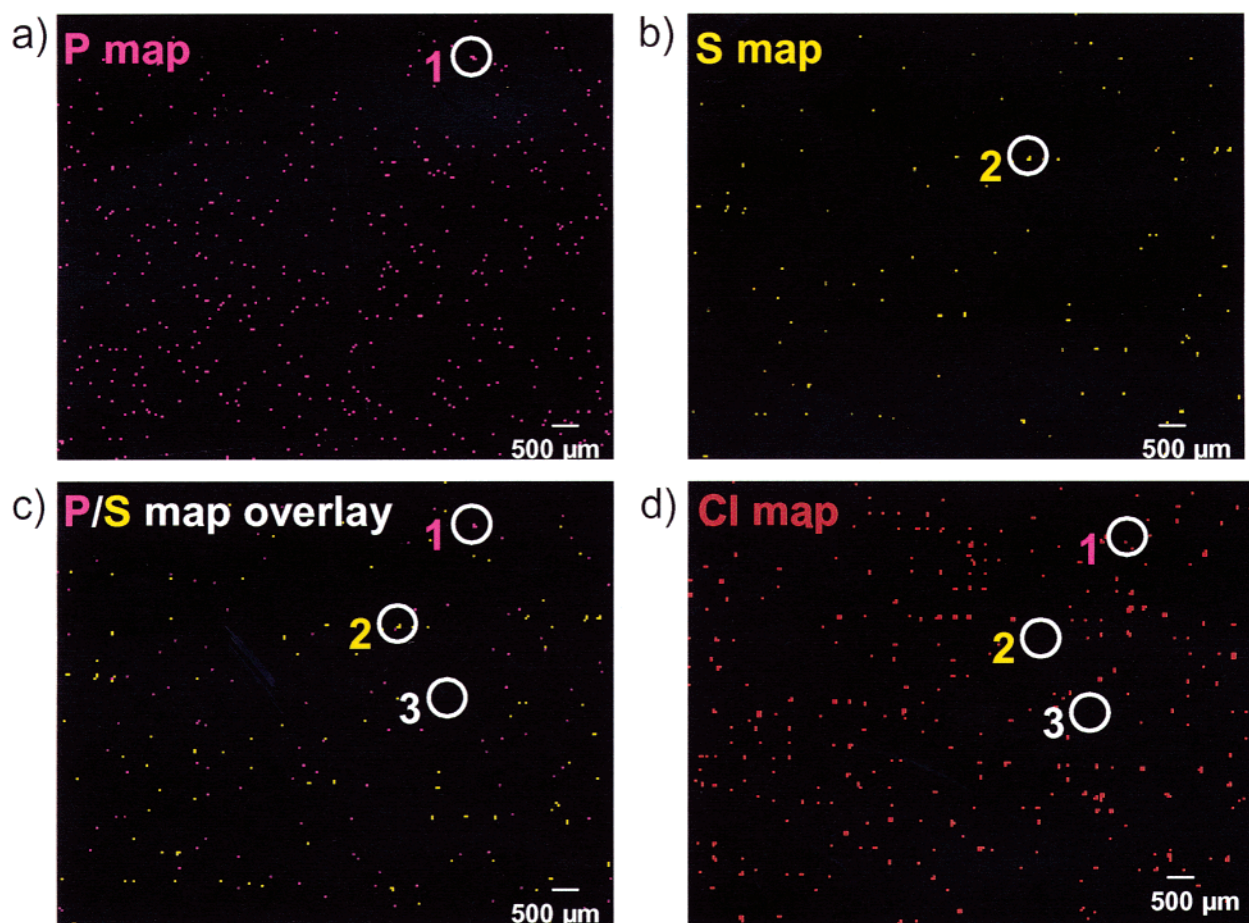


Figure 8. MXRF elemental maps of the exposed oligopeptide combinatorial library to the degradation products of VX 4, 5: (a) P map, (b) S map, (c) P/S overlay map, and (d) Cl map. Bead 1 was selected for sequence analysis because of its high selectivity for binding 4. Similarly, bead 2 was selected for its preferential binding of 5. Bead 3 demonstrated minimal binding for both 4, 5, and Cl.

Table 3. MXRF Cl, P, and S Intensities of CBW Receptor Beads 1, 2, and 3 from the Original Screen and Intensities and Peptide Sequences as Determined from the Verification Experiments

bead <sup>a</sup>	original screen: intensity (counts) <sup>b</sup> , ( <i>n</i> = 1)			sequence	verification: intensity (counts) ( <i>n</i> = 10)		
	Cl	P	S		Cl	P	S
1	5386	530	1214	RGGSGGHGGSF	1208 ± 237	191 ± 45	856 ± 170
2	6214	1181	419	SGGRGGHGGHF	845 ± 257	60 ± 17	908 ± 204
3	7648	552	482	N/A		N/A	

<sup>a</sup> Bead numbers are equivalent to those shown and labeled in Figure 8. <sup>b</sup> P, S, and Cl background intensities (counts) for nonbinding beads in the original screen are P = 561 ± 88, S = 430 ± 55, and Cl = 6628 ± 1082 (*n* = 5).

and these data support what is shown in the P/S overlay. Note that even though the chloride salt of 5 was used in the reaction, bead 2 bound only the thiol amine species, as indicated by the minimal Cl intensity. The sequences of beads

1 and 2, as determined by Edman degradation, are listed in Table 3. These specific immobilized oligopeptides were then subsequently exposed to 4 and 5, and their binding efficiency was verified. Table 3 lists the overall Cl, P, and S intensities



for 10 different beads of each sequence 1 and 2. On the basis of the initial screen in Figure 8, sequence 1 is expected to exhibit high selectivity for **4** (P), whereas sequence 2 was specific for **5** (S). Unexpectedly, the results in Table 3 show that *both* sequences 1 and 2 have a high affinity for **5**. Because of this discrepancy, MALDI-MS was used to verify the sequences of 1 and 2. This discrepancy is puzzling. Obviously, this technique is not immune to false positives. Further experimentation is being pursued to understand this discrepancy and minimize or eliminate any avenues of false positive generation in the technique.

MXRF has shown that both isolated sequences preferentially bind the mercaptoamine. Both peptides have an H amino acid residue in common in the fourth position to the left of the F attachment residue. With this knowledge, a new library can be prepared to find more specific receptors for the mercaptoamine degradation product that keeps the H constant in that fourth position for all sequences. Further experiments to determine better CW receptors are in progress.

### Conclusions

The feasibility of MXRF as a new tool for high-throughput screening was demonstrated through application of catalyst discovery and molecular recognition. The advantages of this nondestructive technique are its speed, sensitivity, and simplicity. Minimal sample preparation is required, and it has the current capability of screening 3200 library components in 1 h or less, depending on the desired sensitivity. At this time, low nanogram quantities of material on the beads can easily be detected. Additionally, no chromogenic tags are needed for analysis. Currently, the MXRF screening technique is at best pseudoquantitative, allowing for some intensity comparison of bound species to be made between combinatorial samples. Current efforts are focused on making the MXRF screen more quantitative so that definite receptor/agent binding ratios can be determined.

The screening methodology can also be improved. Currently, the entire Tacky Dot libraries are mapped by MXRF, including both the combinatorial library beads and the dead space in between. Significant reductions in screening time can be achieved if only the beads are analyzed. This would lead to more rapid scans with higher throughput. The analysis time can be reduced further by using chemometric software. This would be configured to sort through spectra/images to find desired "hits", rather than performing these tasks visually. Efforts are being made to implement these capabilities with the current MXRF technology.

Finally, catalyst/receptor discovery and molecular recognition can be enhanced by using multiple analysis techniques to understand the fundamental chemistry of the library/target

interactions. For example, elemental analysis with MXRF could be coupled to molecular analysis techniques, such as Raman and IR spectroscopies, to study target binding events. The knowledge gained would aid in developing a model for more directed, intelligent library synthesis and screening.

**Acknowledgment.** T.C.M. was supported by the Director of Central Intelligence (DCI) Postdoctoral Research Fellowship Program.

### References and Notes

- (1) Yan, B. *Analytical Methods in Combinatorial Chemistry*; Technomic Publishing Co, Inc.: Lancaster, 2000.
- (2) Orschel, M.; Klein, J.; Schmidt, H. W.; Maier, W. F. *Angew. Chem., Int. Ed. Engl.* **1999**, *38*, 484.
- (3) Cong, P. J.; Doolen, R. D.; Fan, Q.; Giaquinta, D. M.; Guan, S. H.; McFarland, E. W.; Poojary, D. M.; Self, K.; Turner, H. W.; Weinberg, W. H. *Angew. Chem., Int. Ed. Engl.* **1999**, *38*, 484.
- (4) Winograd, N.; Braun, R. M. *Spectroscopy* **2001**, *16*, 14–27.
- (5) Taylor, S. J.; Morken, J. P. *Science* **1998**, *280*, 267.
- (6) Haap, W. J.; Walk, T. B.; Jung, G. *Angew. Chem., Int. Ed. Engl.* **1998**, *37*, 3311–3314.
- (7) Snively, C. M.; Oskarsdottier, G.; Lauterbach, J. J. *Comb. Chem.* **2000**, *2*, 243–245.
- (8) Snively, C. M.; Oskarsdottier, G.; Lauterbach, J. *Catal. Today* **2001**, *67*, 357–368.
- (9) Snively, C. M.; Lauterbach, J. *Spectroscopy* **2002**, *17*, 26–33.
- (10) Snively, C. M.; Katzenberger, S.; Oskarsdottier, G.; Lauterbach, J. *Opt. Lett.* **1999**, *24*, 1841–1843.
- (11) Fischer, M.; Tran, C. D. *Anal. Chem.* **1999**, *71*, 2255–2261.
- (12) Alexander, T.; Tran, C. D. *Anal. Chem.* **2001**, *73*, 1062–1067.
- (13) Senkan, S. M. *Nature* **1998**, *394*, 350.
- (14) Su, H.; Yeung, E. S. *J. Am. Chem. Soc.* **2000**, *122*, 7422.
- (15) Isaacs, E. D.; Marcus, M.; Aeppli, G.; Xiang, X.-D.; Sun, X.-D.; Schultz, P.; Kao, H.-K.; Cargill, G. S., III.; Haushalter, R. *Appl. Phys. Lett.* **1998**, *13*, 1820–1822.
- (16) Carlton, R. A.; Orton, E.; Lyman, C. E.; Roberts, J. E. *Microsc. Microanal.* **1997**, *3*, 520–529.
- (17) Neilly, J. P.; Hochlowski, J. E. *Appl. Spectrosc.* **1999**, *53*, 74–81.
- (18) Yoo, S.-e.; Gong, Y.-D.; Seo, J.-s.; Sung, M. M.; Lee, S. S.; Kim, Y. *J. Comb. Chem.* **1999**, *1*, 177–180.
- (19) Whitehead, D. M.; Jackson, T.; McKeown, S. C.; Wilson, K.; Routledge, A. *J. Comb. Chem.* **2002**, *4*, 255–257.
- (20) Haschke, M.; Klein, J.; Stichert, W.; Vietze, U. *GIT Labor-Fachzeitschrift* **2002**, *46*, 780–782.
- (21) Sun, Y.; Chan, B. C.; Ramnarayanan, R.; Leventry, W. M.; Mallouk, T. E. *J. Comb. Chem.* **2002**, *4*, 569–575.
- (22) Berkessel, A.; Herault, D. A. *Angew. Chem., Int. Ed. Engl.* **1999**, *38*, 102–105.
- (23) Silver, A. *The Biology of Cholinesterases*; North-Holland Publishing Company: Amsterdam, 1974.